Int J Mater Form (2014) 7:179–187
DOI 10.1007/s12289-012-1118-3

ORIGINAL RESEARCH

Characterization of a superplastic aluminium alloy ALNOVI-U through free inflation tests and inverse analysis

D. Sorgente · L. Tricarico

Received: 11 September 2012 / Accepted: 31 October 2012 / Published online: 11 November 2012

Abstract Numerical methods are widespread in forming applications since a deeper understanding and a finer calibration of the process can be reached without most of the assumptions used in analytical approaches. In this calibration procedure the characterization of the material behaviour is an important preliminary step that cannot be avoided. Experimental tests can be numerically modelled and material constants can be found by inverse methods making numerical results as close as possible to experimental ones. In this work material parameters of a superplastic aluminium alloy have been found by experimental forming tests and an inverse analysis. Constant pressure free inflation tests were firstly performed to find the optimal range for temperature and strain rate values. Material constants were then calculated, on the basis of these tests, minimizing errors between experimental and numerical data through a gradient based optimization iterative procedure. Constant strain rate experimental tests were finally used to refine material parameters and to gain a better agreement between experiments and numerical simulations.

Keywords Superplasticity · Inverse analysis · Aluminium alloy

Introduction

Superplastic forming (SPF) is a family of several forming processes involving superplastic (SP) materials. These materials have incredibly high elongations to failure in a specific and narrow range of process parameters such as temperature and strain rate. A controlled microstructure, elevate temperatures (conventionally over a half the absolute melting temperature) and low strain rates are usually requested for *migrograin superplasticity* (the most common type of superplasticity). Due to low strain rates, the forming process of these materials can be not cost-effective especially for mass scale production. However the possibility of reaching elongations much higher than 200 % can bring to significant cost saving benefits: in particular complex shape components can be manufactured without any joint with a weight reduction and an improvements of its mechanical behaviour [1]. Once the initial microstructure is fixed, the SP material should be characterized in order to find optimal conditions in which material offers the highest elongation and the maximum strain rate sensitivity index. In sheet forming of SP materials, these conditions correspond to the best thinning behaviour of the sheet during the manufacturing of complex part. The most common forming technique used in SPF is the gas forming (also called “blow forming” or “cavity forming”) in which the sheet is blown in a female die which has a cavity with the negative shape of the final component. The sheet is constrained between a blank holder (which usually has the gas inflation system) and the female die and no drawing occurs during the forming process. As the strain rate which the sheet undergoes during the forming phenomenon plays an important role in determining material performances, it has to be continuously controlled during the process. The common way of controlling the strain rate, keeping its value in the optimal range, is to change the gas pressure value during the forming process following sheet deformation in the die cavity. Even if several analytical approaches for the strain control exist, they are not practicably achievable when complex shape are desired, as also pointed out by Bonet et al. in a review paper on the simulation of SPF [2]. It’s by now well recognized, both in the industrial and in the academic fields, that finite element (FE) numerical modelling is the simplest and most reliable

D. Sorgente (✉) · L. Tricarico
Dipartimento di Meccanica, Matematica e Management,
Politecnico di Bari,
Viale Japigia 182,
70126 Bari, Italy
e-mail: d.sorgente@poliba.it

solution for calculating the pressure profiling for the SPF process. FE models for the pressure profile prediction need accurate material parameters since the value of the pressure is strictly correlated to the material behaviour, i.e. the strain rate along the sheet during the forming process in turn depends on material constants. Tensile tests are the most widespread method to get superplastic material information, but in the superplastic field several problems can be encountered in the choice of specimen geometry. Moreover cutting accurateness of the specimen is very important and high precision load cells are required. An international standard exists (ISO 20032:2007 [3]) but several different geometries of tensile specimens can be found in scientific papers dealing with tensile tests on SP materials. Different specimen geometries were tested and numerical analysis of the tensile tests in superplastic conditions were performed in [4], denoting that, at elevate temperature and with low flow stress values (both typical of superplastic deformation), some geometrical parameters of the specimen (for instance the value of the fillet radius between the specimen shoulders and the gauge length) could strongly influence measured results much more than in standard tensile tests at room temperature. The material characterization can be done with alternative methods in an easier way and obtaining better results [5–8]. Strain conditions of the forming process can be recreated and material can be tested in a deformation condition that it's much more similar to the forming process one than tensile tests. Enikeev and Kruglov developed a method to gain material constants of a simple constitutive equation by means of two free inflation tests with two different values of the gas pressure [9]. By analytical approximations and geometrical considerations they calculated material constants and achieved a good approximation of the behaviour of a SP titanium alloy in free inflation tests. Sufficiently reliable results can be found by this technique also on other alloys as demonstrated also by the authors [10]. El-Morsy and Manabe numerically simulated a SPF process in a closed die comparing results achieved with material constants from tensile tests and material constants from a multi-dome test, in which the sheet freely expands in cylindrical dies with different diameters [11]. They found a significantly better agreement between experimental and numerical results when using the latter ones. They also demonstrated the importance of taking into account the variation of material constants (the strength coefficient and the strain rate sensitivity index) according to the strain rate.

Without neglecting the physical meaning of material parameters, it is possible to increase FE modelling reliability with a material characterization based on the inverse technique. Material parameters are, in this kind of technique, considered as unknown input variable and calculated by an iterative procedure where also experimental results are considered as an input set of data [12]. Optimization technique are used to minimize errors between numerical results and experiments: starting from a known constitutive equation the goal is to compute the material parameters which minimizes an objective function representing the difference between experimental and numerical data [13]. Experimental results that will be used as reference in the objective function calculation, must be correctly chosen in order to avoid local minima (especially for gradient based optimization technique) and ill-posed problems [12].

In this paper the authors present a work in which the characterization of a SP aluminium alloy was done by results from experimental free inflation tests with the synergic use of a FE numerical model. Both the individuation of the optimal range (of temperature and strain rate) and the material constants evaluation were done by free inflation tests with a laboratory scale equipment. Preliminary constant pressure tests were run to find the optimal temperature and strain rate values. Results of these tests are then used to calibrate a FE numerical model through an inverse technique with a gradient-based method after a wide range exploration phase. Then a constant strain rate pressure law was calculated and applied on the sheet to verify the constitutive equation and to refine the obtained material constants. A variable value of the strain rate sensitivity index was then used in simulation.

Material and experiments

Experiments were performed on aluminium alloy sheets from a single batch. This alloy was purchased in a "superplastic temper" ready for SPF. Laboratory scale equipments were used for the characterization with free inflation tests.

Material

All experiments were performed on a Al-Mg (5XXX series according to Aluminum Association) alloy manufactured by Furukawa-Sky Aluminum Corporation. This alloy is based on the commercial AA5083 alloy but contains a higher Mn weight percentage than the base alloy. Table 1 summarizes the chemical composition of the superplastic Al alloy.

The material is mechanical treated by the manufacturer to have a fine grained microstructure and sold under the commercial name of ALNOVI-U. For this work sheets of 1.35 mm in thickness were purchased in the H18 temper and used in gas SPF tests. Microstructure of the sheet with fine grains is shown in Fig. 1.

The material has a mean grain size of 8.3 μm measured by the linear intercept (Heyn) procedure. In order to decorate the optical microstructure of the material, the specimen was etched in a 10 % phosphoric acid solution at 50 °C in a four steps procedure according to the metallographic technique proposed by Yang [14]. In particular, the aluminium

Table 1 Chemical composition of the superplastic Al- alloy (wt. %)

Si	Fe	Cu	Mn	Mg	Cr	Zn	Ti	Others	Al
0.03	0.06	0.01	1.37	4.60	0.02	-	0.01	< 0.15	Balance

alloy was (i) solution heat treated and water quenched, (ii) aged with a precipitation heat treatment, (iii) polished and over-etched for 15 min in the abovementioned solution and (iv) re-polished to remove etch pitting and etched precipitates in the grain interior. Even though 5XXX aluminium alloys are not classified as heat-treatable alloys this technique gives high contrast in the grain boundary region since precipitates decorate the grain boundaries.

Free inflation tests

The material characterization through free inflation tests was performed on a laboratory scale equipment embedded in the cylindrical split furnace of an INSTRON 4485 universal testing machine. The equipment consists in: (i) a blank-holder, (ii) a female die, (iii) a pneumatic circuit for gas supply with an argon cylinder, proportional electronic valves, steel tubes in the proximity of the forming chamber and flexible polyurethane tubes in colder zones, (iv) an INSTRON electric furnace with its electronic controllers for upper, central and lower zones which can be set with three different temperatures for compensating thermal dispersion, (v) thermocouples to monitor thermal condition on the sheet and on the tools, (vi) a transducer for measuring, during bulging test, the dome height on the specimen and (vii) a PC with a data acquisition I/O device by which pressure, temperature, blank-holder force can be monitored and managed. A schematic representation is given in Fig. 2.

For material characterization, free inflation tests were performed with a cylindrical die cavity (diameter 45 mm with an entry radius of 3 mm) in which the sheet can freely expand; the dome height of the specimen was monitored during the whole test by the acquisition of the position transducer signal.

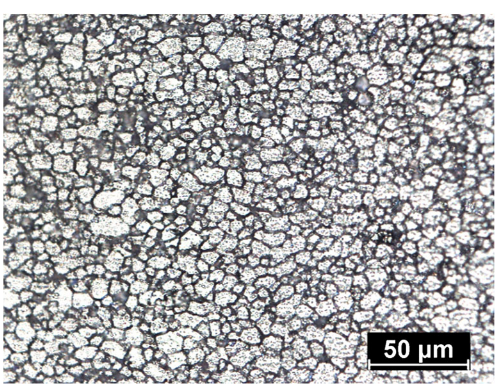

Fig. 1 The microstructure of the fine-grained aluminium alloy ALNOVI-U

Numerical simulations

In this work numerical FE simulation was used for the characterization of the material and for the optimization of rheological parameters. A 2D model of the free inflation test was created and interfaced with an external script able to automatically run simulations with different material constants in order to find the rheological parameters that better fit the real material behaviour.

2D model of free inflation test

A simple axially symmetric numerical model was created using the commercial FE code ABAQUS/Standard with an elastic-viscoplastic integration. The deformable part corresponding to the aluminium blank was divided into 800 continuum elements with 4 nodes and one integration point, the die was considered perfectly rigid and the blank

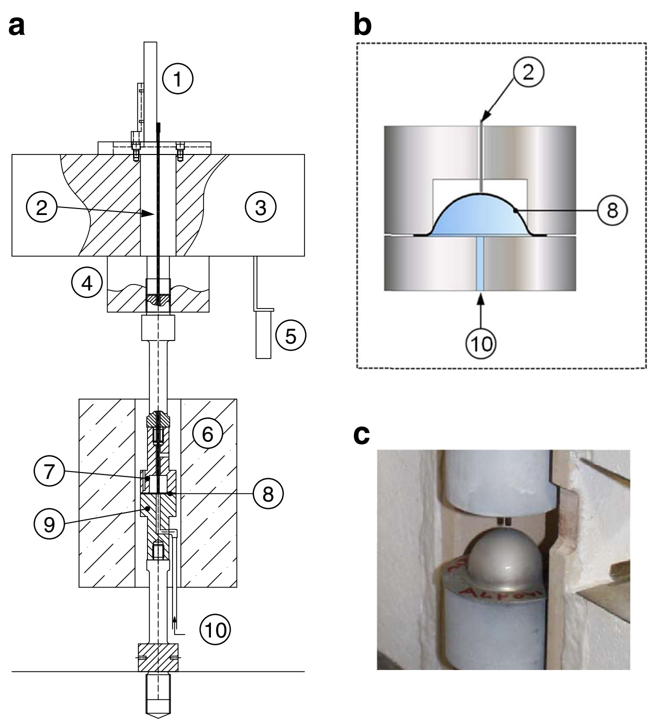

Fig. 2 Equipment for free inflation tests embedded in a universal testing machine with a cylindrical split furnace. **a**) schematic drawing of the whole system: 1) Position transducer for dome height measurement; 2) steel stick for the position transducer; 3) crosshead of the testing machine; 4) load cell; 5) electric fan; 6) cylindrical furnace; 7) die; 8) sheet specimen; 9) blankholder with gas inflation; 10) gas inlet; **b**) particular of the forming chamber; **c**) picture of the deformed specimen after the free inflation test

holder wasn't modelled. The sheet was constrained in its periphery to have no translations and allowing only its thickness variation. The temperature was considered perfectly stable and the material was modelled with the following simple equation:

$$\sigma = C \cdot \dot{\varepsilon}^m \tag{1}$$

where σ is the equivalent flow stress, $\dot{\varepsilon}$ is the equivalent strain rate, C is the strength coefficient and m is the strain rate sensitivity index. In the ABAQUS software for visco-plastic material the CREEP option is available and the equivalent creep strain in the elements is computed by a power law of the equivalent deviatoric stress:

$$\Delta\varepsilon = \dot{\varepsilon} \cdot \Delta t = A \cdot \sigma^n \cdot \Delta t \tag{2}$$

where Δt is time increment in the implicit integration and material constants can be easily related to the ones in Eq. 1: $A = (1/C)^{1/m}$ and $n = 1/m$. Both coefficients can be changed during the deformation according to a state variable that is updated during the simulation using an external FORTRAN subroutine (named USDFLD in ABAQUS [15]). In this work, simulations were run firstly with a constant m value and then with an m value varying as a function of the imposed strain. For pressure profile calculation the internal ABAQUS algorithm (CREEP STRAIN RATE CONTROL) was used to have a fast response and to verify the reliability of material constants found in the characterization.

Inverse technique for material constants determination

The determination of C and m was achieved with a two phases approach: an explorative phase and an optimization phase with a gradient based inverse technique. Gradient based optimization techniques are not very suitable when local minima exist, in fact different solutions could be found starting from different initial values of the variables. Thus, in a first phase, the analysis was focused on the exploration of a wide range of feasible material constants to find a good starting point for the gradient based optimization. To understand if a couple C and m was good in predicting material behaviour, the error between numerical and experimental results was quantified by two objective functions: the smaller these functions the more accurate the numerical result. These functions were based on information not only related to the final strain distribution of the specimen, but, since hot forming applications are strongly affected by time and strain rate, they were built also on time evolution of the deformed shape of the specimen. Therefore, to differentiate good solutions from the bad ones, the evolution of the dome height and of the minimum sheet thickness in free expansion tests were taken concurrently into account. The objective functions Q_h and Q_s, where the subscript h stands for the dome height and the subscript s for thickness, were computed as follows:

$$Q_h = \frac{\sum_{i=1}^{N} \left| \frac{h_{comp}(t_i) - h_{\exp}(t_i)}{h_{\exp}(t_i)} \right|}{N} \tag{3}$$

$$Q_s = \frac{\sum_{i=1}^{M} \left| \frac{s_{comp}(h_i) - s_{\exp}(h_i)}{s_{\exp}(h_i)} \right|}{M} \tag{4}$$

In Eqs. (3) and (4) the subscript *comp* indicates the computed values (from the FE simulation), *exp* the experimental ones obtained by a polynomial interpolation of experimental data, t_i are time values of the frames of the output database of the numerical simulation, N and M are the number of time instants and of the height values considered for the calculations for the dome height h and for the thickness s, respectively. It is not worthless to note that the forming time change significantly according to material parameters. Thus, in order to consider all the experimental values of the thickness, the objective function Q_s is calculated comparing numerical and experimental data at the same height and not at same time instant (s is a function of h in Eq. 4).

The ABAQUS solver is interfaced with a *python* external script which automatically divides a user-defined range of C and m and runs K^2 simulations changing the material constants in the model (K equi-spaced values of the strength coefficient C and K equi-spaced values of the strain rate sensitivity index m). For each simulation, that represent a point of the explored simulation plan, the external script computes the objective functions Q_h and Q_s.

Once this exploration phase is completed, the couple (C, m) at which minimum values of both objective functions are achieved, is used as a starting point for an iterative procedure for the inverse characterization of the material. A schematic illustration of the flowchart of this procedure is given in Fig. 3.

This procedure automatically searched values that give best correlation between the experimental and numerical time evolution of the dome height in the investigated test (reference test). For the minimum seek, the objective function Q_h is considered and the updating of material parameters is done by a gradient based optimization technique. The gradient of the objective function is computed by the finite differences method through the interaction between the python script and the FE solver. This procedure goes on until the objective function is less than a prescribed threshold value or a maximum predefined number of simulations is reached.

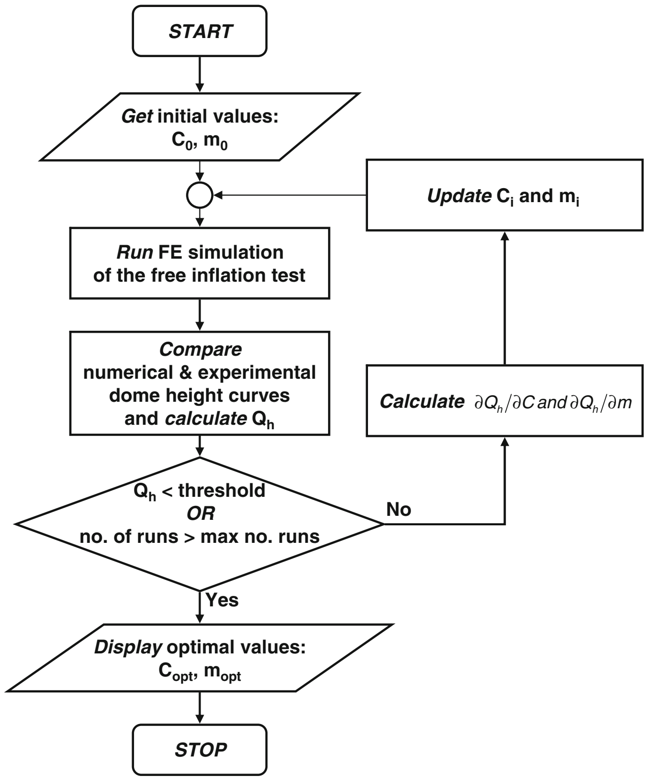

Fig. 3 Flowchart of the inverse procedure for the material constants determination

Results and discussion

In this section results of the forming experiments and of numerical simulations are presented together with the analysis of results. Firstly, constant gas pressure tests were performed in free expansion to locate the best temperature and pressure ranges for material high temperature formability. Then, material constitutive parameters were estimated on the basis of these experimental free inflation tests with constant pressure values. Material constants are lastly refined on the basis of constant strain rates tests that were numerically simulated and then experimentally performed.

Constant pressure tests

An experimental plan was designed and performed varying both temperature and forming gas pressure. According to literature and to the alloy manufacturer guidelines, the optimum forming temperature is around 500 °C. Since in superplastic materials little change in temperature can generate strong difference in values of the elongation to failure, three very close temperature levels (from 480 °C to 520 °C) were investigated changing the pressure from 0.2 to 0.8 MPa. During each test the time evolution of the dome height was acquired and, at the end of the test, the final dome height at failure was measured at room temperature. In Fig. 4 the final dome height at rupture for all the tests at different temperatures and pressure levels is reported.

Since the dome height at failure can be considered a measure of the formability of the material, it can be stated that, in the explored range, the best temperature level is 500 °C and best formability can be achieved in the strain rate range induced by a forming pressure ranging from 0.3 MPa and 0.5 MPa. In Fig. 5 results, in terms of dome height evolution, in this optimal range is reported.

It's well known that a constant pressure test brings to a not constant strain rate in the sheet but, in order to avoid expensive and time-consuming tensile tests, this test can be considered a good starting point for the material characterization. With the aim of estimating the strain rate experienced in the dome apex, the test with 0.4 MPa at 500 °C was repeated stopping the test at different times before failure. In Fig. 6 the thickness and the strain rate values in the dome apex at different time instants are reported together with a picture of the sectioned specimens where the thickness reduction is clearly visible.

The strain rate was approximate to its instantaneous mean value (between experimental measurements) that is calculated as the ratio between the strain variation and the time needed to reach that variation. In the dome apex the strain can be estimated as the natural logarithm of the ratio between the initial and the current value of the thickness. The graph in Fig. 6 clearly shows that the thickness decreased steadily during the test while the strain rate in the dome apex firstly decreased, then flattened out at an almost constant level (about $8\times10^{-4}s^{-1}$) and, at the end, increased again. To a first approximation, it can be stated that the optimal strain rate for this material is not far from $8\times10^{-4}s^{-1}$.

Inverse analysis for material constants estimation

Once optimal temperature and pressure levels were found, the automatic *python* routine was run in order to find material constants. The ranges for the *C* and the *m* values were

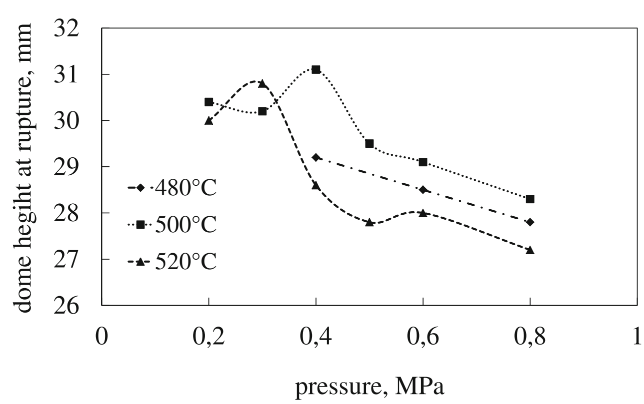

Fig. 4 Dome heights at rupture for tests in the designed experimental plan with different temperatures and pressure levels

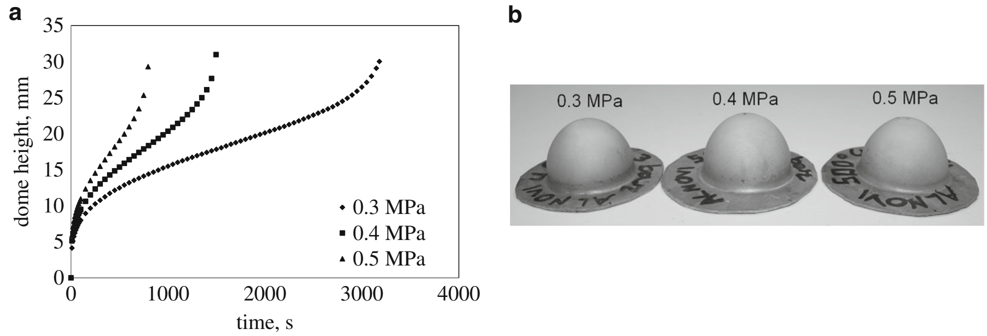

Fig. 5 Dome height evolutions (**a**) and formed specimens (**b**) obtained in the optimal range

set at [100, 910] MPa s^m and at [0.34,0.66] respectively. In this work *K* was set to 10 in order to have a simulation plan of 100 runs which has been considered to give a sufficiently detailed set of data for this exploration phase. The output of the algorithm was an ASCII file that was simply edited by a statistical software for analyzing the distribution of the Q functions versus material parameters interpolating results from the 100 simulations. The reference test, on which the objective functions (Q_h and Q_s) were calculated, was exactly the best condition found in constant pressure tests (0.4 MPa at 500 °C). The whole exploration phase lasted less than 3 h, running on a single processor with a 3.20 GHz frequency. Diagram in Fig. 7 depicts results of this explorative phase with value of the objective functions reported against material constants and minimum areas highlighted with a dotted pattern.

If objective functions are considered separately there are potentially infinite couples of *C* and *m* that gives good results in term of height growth (Q_h) and of thickness evolution (Q_s) prediction. If we look at the objective function build on the height growth (Fig. 7a) we find that a correlation between *C* and *m* exists: either increasing (or decreasing) the m value or decreasing (or increasing) the C value, the height versus time curve change in a very similar way. If we look at the other objective function (Q_s) we can assess that for every value of the strength coefficient C the m value that gives the best prediction is always the same (about 0.5). In Fig. 8 numerical results are compared with experimental ones for different strain rate sensitivity index (ranging between 0.4 and 0.6): the simulation with a value of m equal to 0.5 gives the best prediction especially when large deformation are reached. As the thickness is plotted as a function of the height (and not of the time), the results shown in Fig. 8 can be considered valid for any value of *C*. These results are physically consistent since it is well known the effect of higher values of the strain rate sensitivity index on the diffuse necking phenomenon. A relationship between the thickness and the dome height obtained numerically, by the finite element method, and independent on the C value has already been shown in [16]. Subsequently, it was verified experimentally for different superplastic alloys [6, 17, 18]. Numerical evidence of this behaviour has been highlighted also by Chen et al. [19] in simulation of SPF in a cylindrical die where a relatively higher value of *m* improves the homogeneity of the thickness distribution.

Another results that can be drawn by the observation of Fig. 7 is that the values of Q_s are much lower than values of Q_h. Since the exploration was done on discrete and arbitrary values of material parameters, better results should be found by inverse analysis. Intersecting the areas in the *C*-*m* space where both objective functions have the lowest value, a common region can be found. The common region of these two areas, where the material constants can suitably predict material behaviour, was considered for the succeeding inverse analysis. Thus, with the aim of refining material parameters, values of *C* and *m* of the common region (250.0 MPa s^m and 0.5 respectively) were considered as the initial values for the gradient based iterative procedure of the inverse analysis described in previous sections with a threshold value of Q_h equal to 5 % and a maximum number

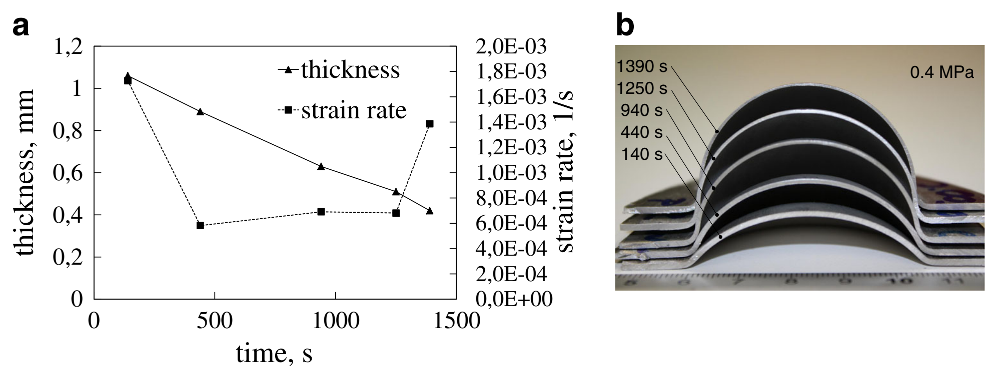

Fig. 6 Thickness and strain rate evolution in the dome apex during the test at 500 °C with a constant pressure of 0.4 MPa (**a**) and sectioned specimens for the thickness acquisition (**b**)

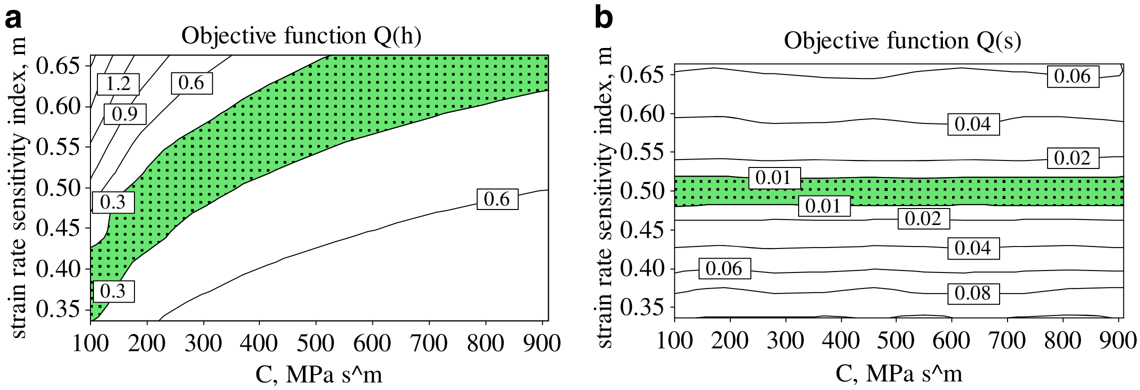

Fig. 7 Contour plots of the objective function Q_h (**a**) and Q_s (**b**) where the minimum area are highlighted with a dotted pattern

of runs equal to 100. In Table 2 the values of *C* and *m* during different phases of the inverse analysis run after the exploration phase are summarized.

The last row of Table 2 refers to the end of the iterative procedure that, in this case, ended since the maximum number of runs was reached without getting the value of Q_h under the threshold value (it is sufficient that one of these two conditions is verified, so that the iterative procedure is stopped as shown in the flowchart reported in Fig. 3).

It can be found that, whether for the objective function build on the thickness values the final error was very small (Q_s value less than 1 %), the Q_h did not go under a value of 6.6 %. This was considered as a direct consequence of the constitutive equation used to represent the material behaviour, where *C* and *m* values were constant even if it was demonstrated that, especially, for 5XXX aluminium alloys it's a too strong approximation [20]. This will showed also in the next section where a constitutive model with a variable m is described.

With the new values of *C* and *m*, derived from inverse analysis, new simulations and experimental tests with an optimized pressure law able to keep the strain rate value at a constant value were performed as described in the following section.

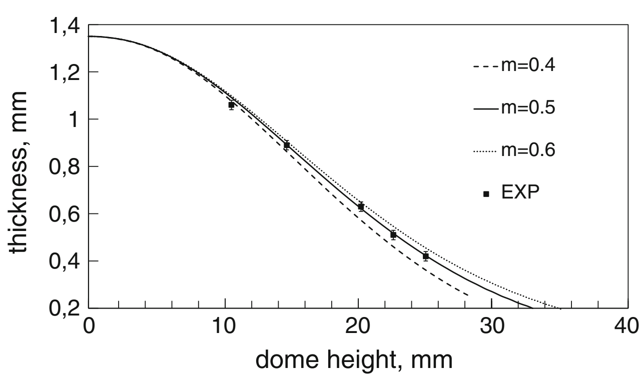

Fig. 8 Thickness evolution in the dome apex during the test at 500 °C with a constant pressure of 0.4 MPa calculated with different strain rate sensitivity index values and compared with the experimental one

Constant strain rate free inflation test

The ABAQUS internal algorithm able to control the strain rate was applied to the whole sheet in the 2D numerical model in order to achieve a pressure profile able to keep the maximum strain rate close to the strain rate value $8\times10^{-4}s^{-1}$. As already highlighted in previous sections, this value was found, in constant pressure tests, as the strain rate value that brought to the highest dome height at failure. The *C* and *m* value found by the inverse analysis were implemented in the numerical model and considered, in this first phase, constants over the forming process. The so achieved pressure profile was used, after polynomial interpolation, in a free inflation experimental test. Results revealed that the correspondence between numerical and experimental tests were not satisfactory especially for the time evolution of the dome height (Fig. 9a). In particular, while in the first phase of the test the experimental height was higher than the numerical one, in the final part of the test the experimental height rate was lower than numerical one and the final dome height is significantly lower than the computed one (the failure of the specimen was not achieved in this experimental test stopped at 2800 s). This phenomenon is in accordance with results showed in a paper by Ridley et al. [20] where, by means of jump tensile tests, they demonstrated that, while for a 7XXX superplastic aluminium alloy the *m* value was almost constant as the strain increased, for a 5XXX superplastic aluminium alloy the *m* value decreased with increasing strain. In fact, in free inflation tests, at constant pressure, it can found that the higher the *m* value the higher the dome height grow rate. Similar results was found also by the authors [21]

Table 2 *C*, *m* and objective functions during the inverse analysis

Phase	C [MPa s^m]	m	Qh	Qs
Initial	250.0	0.5000	9.0 %	0.9 %
First Iteration	247.2	0.5000	7.5 %	0.9 %
Last Iteration	244.1	0.5000	6.6 %	0.9 %

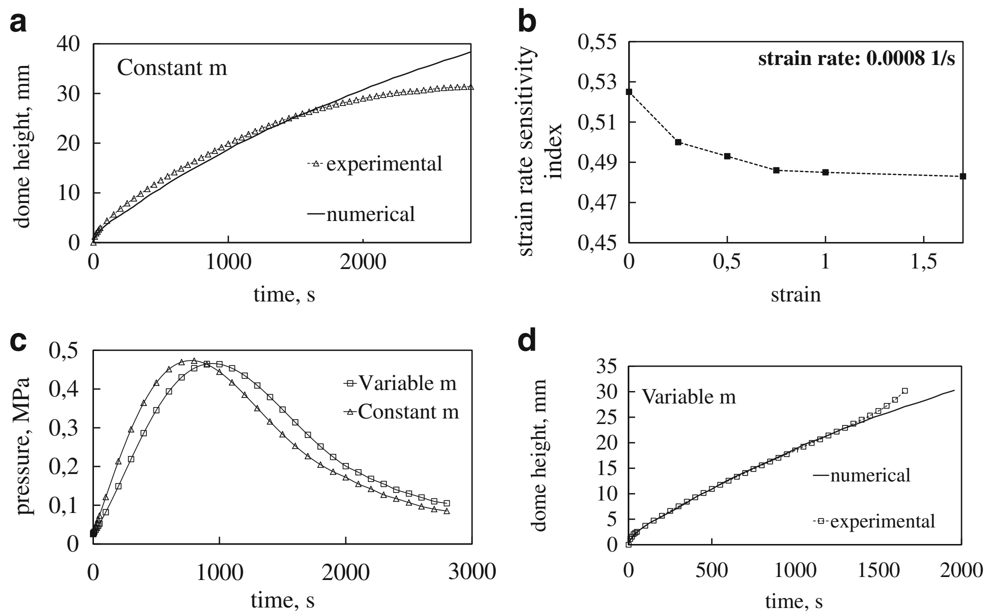

Fig. 9 Dome height evolutions (**a** and **d**) and pressure profiles (**c**) obtained considering both a constant and a variable m (**b**) value during simulation with a constant strain rate of $8\times10^{-4}\,s^{-1}$

on a similar 5XXX Al alloy and on a AZ31 Mg alloy where the variable *m* value was calculated by an analytical approach and by results of free inflation tests with pressure jumps during the test. Following this concept, the ALNOVI-U behaviour was modelled, for the constant strain rate inflation test, as a function of the strain, i.e. the strain rate sensitivity index decreased with the strain. The evolution of the *m* value was found by inverse analysis keeping constant the strength coefficient *C* and vary the *m* value in order to achieved a numerical height evolution close to the experimental one in the constant strain rate test (Fig. 9b).

In their paper, Ridley et al. stated and demonstrated also that, even jump tensile tests highlighted that the strain rate sensitivity index decreased with the strain, this state variable (i.e. the strain) must be replaced with other ones based on microstructural parameters to have a good prediction of the material behaviour at different strain rates. Nevertheless, in a constant strain rate condition, this approximation (using the strain as a state variable) can be considered valid and can give a sufficiently affordable material behaviour prediction.

Once this m-law was found, the 2D simulation was run again with this new constitutive law. A new pressure law was calculated by the ABAQUS algorithm (keeping the target strain rate at the same value of the previous simulation) and the experimental test repeated with this new pressure profile. Pressure–time and dome height-time curves are reported in Fig. 9c and d.

It's possible to observe that the variable strain rate sensitivity index is not far from the constant value of *m* achieved in the inverse calibration but, since the time evolution of the dome height is strongly dependent on the *m* value, a small variation of this material parameter brought to a significant variation of the height versus time curve without significantly affecting the thickness distribution. A better agreement was found modelling the material with a variable *m* value, especially for height values under 25 mm. This height value corresponds to an equivalent strain value of about 1.2. It's not worthless to note that, in this work, the constitutive equation, even with a variable *m*, did not take into account cavitation and this can be one of the main reason of bad correlation between experiments and simulations for strain values close the material failure. Considering that in most industrial SPF applications, the deformation is never brought to values close to failure, achieved results may be considered to be of interest also for the simulation of industrial applications.

Conclusions

With the aim of creating a reliable numerical model able to give optimal pressure profiles for a superplastic forming process, the commercial superplastic aluminium alloy ALNOVI-U was characterized by means of free inflation tests. The optimal temperature and pressure range was found at 500 °C and between 0.3 and 0.5 MPa, respectively. The corresponding strain rate value, that was estimated by thickness measurement during free inflation tests, was $8\times10\text{-}4\ s^{-1}$. An inverse analysis was run for estimating material parameters; main results of this analysis were (i) the strain rate sensitivity index strongly influences the thickness evolution during the free inflation test, (ii) the correlation between the experimental height with the numerical one was not satisfactory with a constant value of the strain rate sensitivity index m. Results achieved demonstrated that, even with a simple constitutive equation, it is possible to characterize a new superplastic material without tensile tests. Numerical simulations and inverse analysis could, especially if the physics of the problem is neglected, bring to inconsistent results but, especially for new materials and hard to set process can give a huge help in the understanding of the forming phenomenon. For a more accurate and wide characterization, the constitutive equation should consider other state variables (microstructural one for instance) in order to catch material behaviour in a wider range of strain and strain rate values.

Acknowledgments The authors wish to thank the Italian Institutions Region APULIA and MIUR (Ministry of Education, University and Research) for financing the present research activity (TRASFORMA and SMATI projects).

References

1. Chandra N (2002) Constitutive behavior of superplastic materials. Int J Non Lin Mech 37:461–484
2. Bonet J, Gil A, Wood RD, Said R, Curtis RV (2006) Simulating superplastic forming. Comput Meth Appl Mech Eng 195(48–49):6580–6603
3. ISO 20032:2007 - Method for evaluation of tensile properties of metallic superplastic materials
4. Sorgente D, Tricarico L (2007) Analysis of different specimen geometries for tensile tests in superplastic conditions for an aluminium alloy. Mater Sci Forum 551–552:123–128
5. Carrino L, Giuliano G, Polini W (2003) A method to characterise superplastic materials in comparison with alternative methods. J Mater Process Technol 138(1–3):417–422
6. Giuliano G (2009) Thickness and strain rate at the sheet dome apex in superplastic bulge forming tests. Int J Mater Form 2(1):375–378
7. Franchitti S, Giuliano G, Palumbo G, Sorgente D, Tricarico L (2008) On the optimisation of superplastic free forming test of an AZ31 magnesium alloy sheet, Int J Mater Form Suppl 1:1067–1070
8. Kappes J, Wagner S, Schatz M (2010) Superplastic sheet metal forming with focus on the warm bulge test and its in-process monitoring. Int J Mater Form 3(1):1135–1138
9. Enikeev FU, Kruglov AA (1995) An analysis of the superplastic forming of a thin circular diaphragm. Int J Mech Sci 37(5):473–483
10. Sorgente D, Scintilla LD, Palumbo G, Tricarico L (2010) Blow forming of AZ31 magnesium alloy at elevated temperatures. Int J Mater Form 3:13–19
11. El-Morsy AW, Manabe KI (2002) FE simulation of rectangular box forming using material characteristics from the multi-dome test. J Mater Process Technol 125–126:772–777
12. Liu GR, Han X (2003) Computational inverse techniques in non-destructive evaluation. CRC Press
13. Gavrus A, Massoni E, Chenot JL (1996) An inverse analysis using a finite element model for identification of rheological parameters. J Mater Process Technol 60(1–4):447–454
14. Yang HS (1997) A new light optical metallographic technique for revealing grain structures of common 2000, 5000, and 7000 series aluminum alloys. Mater Charact 38(3):165–175
15. Abaqus User Subroutines Reference Manual, Version 6.10, section 1.1.45 User subroutine to redefine field variables at a material point. Dassault Systèmes, 2010
16. Giuliano G, Franchitti S (2007) On the evaluation of superplastic characteristics using the finite element method. Int J Mach Tool Manuf 47:471–476
17. Giuliano G (2012) Superplastic Constitutive Modelling of AA-5083. TECHNISCHE MECHANIK 32(2–5):221–226
18. Giuliano G (2012) AZ31 Magnesium Alloy Parameters Identification through Inverse Analysis at 713 K. Key Engineering Materials 504–506:643–646
19. Chen Y, Kibble K, Hall R, Huang X (2001) Numerical analysis of superplastic blow forming of Ti-6Al-4V alloys. Mater Des 22:679–685
20. Ridley N, Bate PS, Zhang B (2005) Material modelling data for superplastic forming optimisation. Mater Sci Eng, A 410–411:100–104
21. Sorgente D, Palumbo G, Tricarico L (2007) Material superplastic parameters evaluation by a jump pressure blow forming test. Key Engineering Materials 344:119–126